# Selection rules and linear absorption spectra of carbon nanotubes in axial magnetic fields

Hong Liu,[1,2] Stefan Schumacher,[2] and Torsten Meier[2]

[1]*Physics Department, Nanjing Normal University, Nanjing 210046, China*

[2]*Department of Physics and CeOPP, University Paderborn, Warburger Straße 100, D-33098 Paderborn, Germany*

(Received 26 March 2013; revised manuscript received 1 June 2013; published 16 July 2013)

We derive a transparent and easy-to-use analytic expression for the selection rules and the optical dipole matrix elements for carbon nanotubes of arbitrary chirality in the presence of axial magnetic fields using a single-orbital $\pi$-electron tight-binding model. From this, we calculate the linear absorption spectrum for arbitrary polarization directions of the incident light, providing insight into all optically allowed transition. We show that the transverse absorption peaks can be selectively excited with circularly polarized light and spectrally resolved in an axial magnetic field.

DOI: 10.1103/PhysRevB.88.035429 PACS number(s): 78.67.−n, 78.67.Ch, 78.67.Bf, 73.22.−f

## I. INTRODUCTION

Since the discovery of carbon nanotubes (CNTs),[1] the optical properties of CNTs have extensively been analyzed, both in experimental and theoretical studies. In particular, due to the quasi-one-dimensional characteristic of CNTs, the linear absorption[2–6] and excitonic resonances[7–12] have been theoretically investigated for light polarized parallel to the nanotube axis. Among the previous theoretical work on dipole matrix elements, Ajiki and Ando[5] derived the selection rules and simple expressions for the dipole matrix elements in effective-mass approximation. This approach, however, neglected higher-order effects, which are important for the so-called family effects in the optical absorption spectra.[9,13–16] Malić *et al*. reported an analytic expression of the momentum matrix elements using a tight-binding method but considered only for incident light parallel polarized parallel to the tube axis.[2] Recently, the absorption coefficient of CNTs for light with arbitrary polarization directions with respect to the nanotube axis has been measured, and the optical cross section varying with nanotube chirality was obtained.[17–20] The optical properties of CNTs for cross-polarized light were studied theoretically, and selection rules were obtained analytically.[21–26] Zarifi *et al*.[24] derived an analytic but complicated expression for the dipole matrix elements and obtained selection rules for the polarization perpendicular to the nanotube axis.

Thus, until now, a simple formula for the vectorial dipole matrix elements has not been presented. Here, we derive such a simple analytic expression for the dipole matrix elements for arbitrary polarization directions of the incident light field. We also generalize and apply the expression to systems including an applied axial magnetic field. Based on our results, detailed insight is obtained about every peak in the linear absorption spectrum of various types of CNTs in the presence and absence of axial magnetic fields. Especially when an axial magnetic field is applied, a splitting in the nanotube's band structure occurs such that, with circularly polarized light, certain band-to-band transitions can be selectively excited. Since excitons are superpositions of band-to-band transitions,[27,28] the results presented here will also appear in the excitonic absorption and thus should be observable.

## II. SELECTION RULES AND OPTICAL DIPOLE MATRIX ELEMENTS

We start with the definition of the interband dipole matrix elements[29]

$$\mathbf{M}^{cv}(\mathbf{k}) = \frac{-e\left\langle \psi_k^c \right| \hat{H}\mathbf{r} - \mathbf{r}\hat{H} \left| \psi_k^v \right\rangle}{E_k^c - E_k^v}, \tag{1}$$

where $\hat{H}$ is the Hamiltonian of the system, and $\psi_k^c(\psi_k^v)$ and $E_k^c$ $(E_k^v)$ are the wave functions and the energies of the conduction band $c$ (valence band $v$) at a given $k$-vector for the transition $v \to c$, respectively. Within a single-orbital $\pi$-electron tight-binding model, the Hamiltonian is given by

$$\hat{H} = \sum_{\langle i,j\rangle,s} (t_{ij} C_{is}^{+} C_{js} + h.c.), \tag{2}$$

where the summation $\langle i,j\rangle$ runs over nearest-neighbor sites only, $C_{is}^{+}(C_{is})$ is the electron creation (annihilation) operator at site $i$ with spin $s$. According to the gauge invariance, the hopping matrix element in the presence of magnetic field $\mathbf{B}$ can be expressed as $t_{ij} = t_0 \exp(i\frac{2\pi}{\phi_0}\int_{\mathbf{r}_i}^{\mathbf{r}_j} \mathbf{A}\cdot d\boldsymbol{l})$ between two sites $i$ and $j$ by using the vector potential $\mathbf{A}$. Here, $\phi_0 = hc/e$ is the magnetic flux quantum. The unit vectors and the bond vectors of the graphene lattice are shown in Fig. 1.

When applying a magnetic field $\mathbf{B}$ along the tube axis, the discrete $k$-vectors along the circumference are shifted and given by $k_c = 2\pi(l + k_H)/(c_h a)$ with the ratio $k_H = B\pi R^2/\phi_0$ between the magnetic flux through the cross-sectional area $\pi R^2$ of the CNT and the magnetic flux quantum $\phi_0$. Here, $c_h = \sqrt{n^2 + nm + m^2}$, $a = 0.2416\,nm$, and $R$ is the tube's radius. The hopping parameters along the three

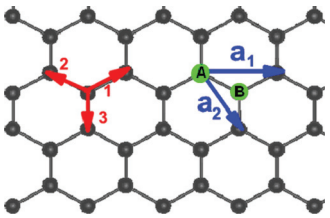


FIG. 1. (Color online) Lattice structure of graphene including the unit vectors and three bond vectors.

 

bond vectors are given by $t_1 = t_0 e^{ik_H\varphi_n}$, $t_2 = t_0 e^{-ik_H\varphi_{n+m}}$, and $t_3 = t_0 e^{ik_H\varphi_m}$, where $t_0 = -3.00\,eV$, $\varphi_l = l\pi/c_h^2$, and $\alpha_j = j2\pi/N_h$, where $N_h$ is the total number of graphene cells in one CNT unit cell. The electronic dispersions within each band with index $l$ is $E_{lk} = \pm|t_0||g_{lk}|$ and $g_{lk} = e^{i\vec{k}\cdot\vec{d}_1} + e^{i\vec{k}\cdot\vec{d}_2} + e^{i\vec{k}\cdot\vec{d}_3}$, in which $\vec{d}_1$, $\vec{d}_2$, and $\vec{d}_3$ are the three bond vectors pointing from the site $B$ atom to the three nearest-neighbor sites ($A$ atoms) shown in Fig. 1. For tubes with indices $(n, m)$ in an applied axial magnetic field, the energy dispersions can be written as[30]

$$E_{lk} = \pm|t_0|\sqrt{3 + 2\cos(\varphi_{(2n+m)(l+k_H)} + \alpha_{mk}) + 2\cos(\varphi_{(n+2m)(l+k_H)} - \alpha_{nk}) + 2\cos(\varphi_{(n-m)(l+k_H)} + \alpha_{(m+n)k})}. \quad (3)$$

Subsequently, in nearest-neighbor approximation, we can write the dipole matrix elements in Eq. (1) explicitly as[6,24]

$$\mathbf{M}^{cv}_{ll'}(k) = \frac{-e}{\left(E^c_{lk} - E^v_{l'k}\right)N_h}\sum_{n=0}^{N_h-1}\sum_{m=1}^{3}\left[c^{c^*}_{lk,B}c^v_{l'k,A}t_{nA,m}e^{i\mathbf{k}\cdot(\mathbf{r}_{nA}-\mathbf{r}_{mB})}(\mathbf{r}_{nA} - \mathbf{r}_{mB}) + c^{c^*}_{lk,A}c^v_{l'k,B}t_{nB,m}e^{i\mathbf{k}\cdot(\mathbf{r}_{nB}-\mathbf{r}_{mA})}(\mathbf{r}_{nB} - \mathbf{r}_{mA})\right]. \quad (4)$$

Here, $\mathbf{r}_{mB}(\mathbf{r}_{mA})$ denotes the coordinates of the three nearest-neighbor sites of site $\mathbf{r}_{nA}(\mathbf{r}_{nB})$. Also, $c^c_{lk,i}$ and $c^v_{lk,i}$ are the expansion coefficients at site $i$ of the eigenstates of conduction $c$ and valence bands $v$ at each $k$-vector with the band index $l$ ($l = 0,1,2\cdots,N_h - 1$), respectively.

For the coordinate component $(\mathbf{r}_i)_c$ along the circumference at site $i$ of the CNT, we introduce $r_i^{\pm} = x_i \pm iy_i$, such that $(\mathbf{r}_i)_c = \frac{1}{2}r_i^+(\mathbf{e}_x - i\mathbf{e}_y) + \frac{1}{2}r_i^-(\mathbf{e}_x + i\mathbf{e}_y)$. Substituting this expression into Eq. (4), we arrive at a fairly simple analytic form for the dipole matrix elements

$$\mathbf{M}^{cv}_{ll'}(k) = \frac{-e\,t_0}{E^{cv}_{lk,l'k}}\left[2\mathrm{Re}\left(c^{c^*}_{lk,B}c^v_{lk,A}z_{lk}\right)\mathbf{e}_z\delta_{ll'} + iR\mathrm{Im}\left[c^{c^*}_{lk,B}c^v_{l'k,A}\left(g_{lk} - g_{l'k}\right)\right](\mathbf{e}_x \pm i\mathbf{e}_y)\delta_{l\pm1,l'}\right], \quad (5)$$

where $E^{cv}_{lk,l'k} = (E^c_{lk} - E^v_{l'k})$, $c^c_{lk,A} = -c^v_{lk,A} = (c^{c(v)}_{lk,B})^* = \sqrt{g_{lk}/(2|g_{lk}|)}$, and the coefficient $z_{lk} = d_{1z}e^{i\vec{k}\cdot\vec{d}_1} + d_{2z}e^{i\vec{k}\cdot\vec{d}_2} + d_{3z}e^{i\vec{k}\cdot\vec{d}_3}$. Moreover, for a $(n, m)$ tube in an applied axial magnetic field where the strength is expressed by the parameter $k_H$, the coefficients at $k$-vector $(l, k)$ can be written as

$$g_{lk} = e^{i(n\varphi_{(l+k_H)} + \frac{n+2m}{3}\alpha_k)} + e^{i(-(n+m)\varphi_{(l+k_H)} + \frac{n-m}{3}\alpha_k)} + e^{i(m\varphi_{(l+k_H)} - \frac{2n+m}{3}\alpha_k)},$$

$$z_{lk} = \frac{a}{2\sqrt{3}c_h}\left[(n+2m)e^{i(n\varphi_{(l+k_H)} + \frac{n+2m}{3}\alpha_k)} + (n-m)e^{i(-(n+m)\varphi_{(l+k_H)} + \frac{n-m}{3}\alpha_k)} - (2n+m)e^{i(m\varphi_{(l+k_H)} - \frac{2n+m}{3}\alpha_k)}\right].$$

The integer $k$ lies in the interval $-\frac{N_k}{2} \leqslant k < \frac{N_k}{2}$.

Compared with previous studies,[2,5,6,24] the present analytical expression is significantly simpler, clearly shows the selection rules, and allows one to easily obtain the value of the dipole matrix elements for arbitrary polarization directions of the incident light. Especially the $x$ and $y$ components are much simpler than the expressions given in Ref. 24. As can be seen in Eq. (5), the longitudinal $z$ component is real-valued. The $x$ and $y$ components can give rise to a complex-valued contribution with a relative phase between them. The symmetry relation $M_y^{\pm} = \pm iM_x^{\pm}$ and the angular momentum selection rule $\delta_{l\pm1,l'}$ give rise to transitions that can be excited with circularly polarized light propagating along the tube axis. The symmetry $M^{l,l\pm1}_{x(y)} = -M^{l\pm1,l}_{x(y)}$ holds for the two transverse dipole matrix elements $M^{l,l\pm1}_{x(y)}(l \to l \pm 1)$ and $M^{l\pm1,l}_{x(y)}(l \pm 1 \to l)$.

In agreement with earlier studies,[2–15,21–27] we recover the essential selection rule: $\Delta l = 0$ for optically allowed transitions for $z$-polarized light (polarized along the tube axis). The selection rule $\Delta l = \pm1$ is found for the optically allowed transitions for light polarization directions perpendicular to the tube axis. In the limiting case of a circularly polarized beam propagating along the tube axis $\mathbf{e}^{\pm} = \mathbf{e}_x \pm i\mathbf{e}_y$, the selection rule $l \to l \pm 1$ has to be obeyed for optical transitions such that certain transitions can be selectively excited.

For parallel-polarized excitation, by using $\gamma_{lk} = \arctan[\mathrm{Im}(g_{lk})/\mathrm{Re}(g_{lk})]$ the $z$ component of dipole matrix element can be simplified to

$$M_z^{cv}(l,k) = \frac{-e}{2|g_{lk}|}\mathrm{Re}(e^{i\gamma_{lk}}z_{lk})\delta_{ll'}. \quad (6)$$

This formula is in agreement with Ref. 2. In particular, for an achiral zigzag tube $(n,0)$, $E_{lk} = \pm|t_0|\sqrt{1 + 4\cos\theta_l(\cos\theta_l + \cos3\beta_k)}$ with $\theta_l = (l + k_H)\pi/n$ and $\beta_k = k\pi/3$, the longitudinal $z$ component of the dipole matrix elements is found to be

$$M_z^{cv}(l,k) = \frac{ea}{2\sqrt{3}}\frac{\cos2\beta_k\cos2\theta_l - \cos\beta_k\cos\theta_l + 2\sin\beta_k\sin3\beta_k}{4\cos\theta_l(\cos\theta_l + \cos3\beta_k) + 1}. \quad (7)$$

The $z$ components of the dipole matrix elements for all zigzag tubes has the following symmetry with respect to the $\Gamma$ point, i.e. $M_z(-k) = M_z(k)$.

## III. RESULTS AND DISCUSSION

The analytic results for the dipole matrix elements presented above are of a general nature. As an example, in

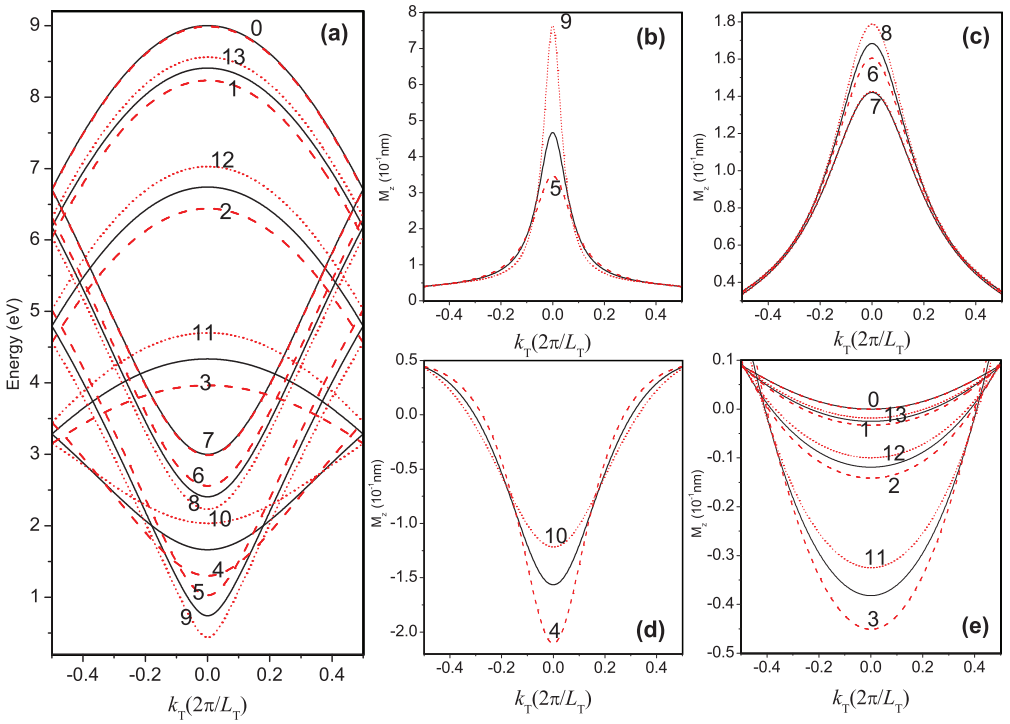


FIG. 2. (Color online) The band structure and the longitudinal $z$ components of all dipole matrix elements for tube (7,0) without and with magnetic field, respectively. (a) Band structure without and with magnetic field. The origin on the vertical energy axis lies in the middle of the electronic gap separating valence and conduction band states. (b)–(e) The dipole matrix elements. The black solid lines are for $k_H = 0$. The red lines are for $k_H = 0.14$, where the red dotted lines correspond to the bands 8–13 and the red dashed lines correspond to the bands 0–7, respectively. The numbers denote the band indices.

the following paragraphs, we specifically discuss results for a typical semiconducting (7, 0) CNT. Results for the band structure and the dipole matrix elements are shown in Figs. 2 and 3. Only the band structure for the conduction band is shown in Fig. 2 because of the conduction-valence-band symmetry. The dipole matrix elements vary with the parameter $k_H$. The splitting of the twofold degenerate bands caused by an applied magnetic field also influences the corresponding dipole matrix elements. No change occurs for dipole matrix elements between nondegenerate bands, such as the bands 7 and 0 for tube (7, 0) in Fig. 2. For this semiconducting zigzag tube, the splitting caused in the dipole matrix elements by the magnetic field is similar to that found in the band structure. The two dipole matrix elements, which are identical without a magnetic field, separate around the original one. This is true both for the longitudinal $z$ as well as the transverse $x$ and $y$ components.

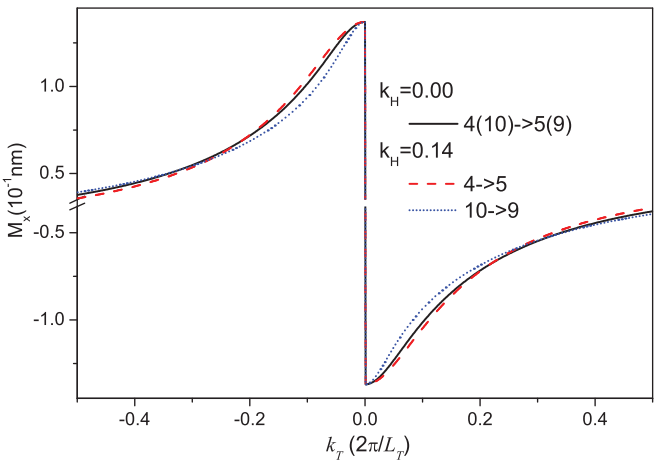


FIG. 3. (Color online) The transverse $x$ components of the dipole matrix elements corresponding to the lowest-frequency peak for the (7, 0) zigzag tube with and without magnetic field. The numbers refer to the indices of the involved bands.

In Fig. 3, we show the dipole matrix elements for the lowest-frequency transverse transitions: $4 \rightarrow 5$ and $10 \rightarrow 9$. The related elements $5 \rightarrow 4$ and $9 \rightarrow 10$ can be obtained using the symmetry relation $M_x^{l,l'} = -M_x^{l',l}$. Visible is the inversion symmetry at the $\Gamma$ point, i.e. $M_x^{l,l'}(-k) = -M_x^{l,l'}(k)$, which is not present for the $z$ components of the dipole matrix elements. The maximum value of the $x$ components of the dipole matrix elements is about one fourth of the maximum value of the $z$ components. The applied magnetic field only leads to a small splitting in these transverse components.

## IV. LINEAR ABSORPTION SPECTRA

Most of the previous theoretical studies concentrated on the linear absorption for perpendicular or parallel-polarized light fields.[2–6,20–26] We note the experimental work on the optical spectra[31] and polarization-dependent magneto-absorption for CNTs with magnetic fields,[32] but as far as we know, the circular-polarized absorption experiment in the absence or presence of magnetic field has not been reported.

In the linear optical regime, the optical absorption spectrum can directly be obtained as a sum over all resonant contributions from optically induced interband transitions separately

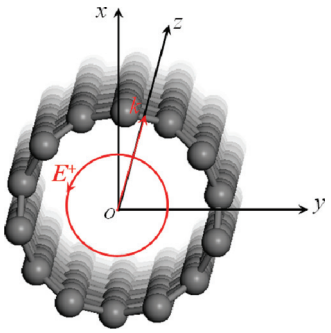


FIG. 4. (Color online) The sketch of the right circularly polarized laser in tube (7, 0).

for each frequency and $k$-vector. The analytic expression of the optical absorption spectrum then takes the general form[3,4,24,28]

$$\alpha(\omega) \approx \omega \sum_{lk,l'k} \left|\mathbf{e}_E \cdot \left(\mathbf{M}^{cv}_{lk,l'k}\right)^*\right|^2 \frac{\gamma}{\left(\hbar\omega - E^{cv}_{lk,l'k}\right)^2 + \gamma^2}, \quad (8)$$

with the transition energy $E^{cv}_{lk,l'k} = E^c_{lk} - E^v_{l'k}$ of each band-to-band contribution. Here, $\mathbf{e}_E$ is the polarization direction of the incident laser. Lorentzian homogeneous broadening is included with $\gamma = 0.01$ eV. Using our analytic expression, the parallel-polarized linear absorption spectra for zigzag tubes are identical to the theoretical results obtained previously.[2]

For a perpendicularly polarized incident laser, the dominant absorption peaks stem from four transitions: $l \leftrightarrow l \pm 1$ and $l' \leftrightarrow l' \pm 1$, in which $l$ and $l'$ are the band indices of the twofold degenerate band, cf. Refs. 19–24. When applying an axial magnetic field, the absorption peak splits into two peaks: one for the two transitions $l \leftrightarrow l \pm 1$ and another one for $l' \leftrightarrow l' \pm 1$. Next, we study the circularly polarized linear absorption spectrum according to the selection rules $l \to l \pm 1$ in Eq. (5). For the right circularly polarized laser $\mathbf{e}^+ = \mathbf{e}_x + i\mathbf{e}_y$ in the circumference plane shown in Fig. 4, every absorption peak is attributed mainly to two optically allowed transitions: $l \to l + 1$ and $l' \to l' + 1$. If further applying a magnetic field along the tube's axis, the peak splits into two peaks corresponding to only a single transition each: $l \to l + 1$ and $l' \to l' + 1$, respectively. Therefore, the transverse absorption peaks can be selectively excited with circularly polarized light and appear as spectrally separate resonances in an axial magnetic field.

We take the zigzag tube (7, 0) as an example to show the right circularly polarized linear absorption spectrum in Fig. 5. In the absence of a magnetic field, the first (lowest frequency) peak originates from only two transitions: $4 \to 5$ and $9 \to 10$. The other two transitions $5 \to 4$ and $10 \to 9$ are optically forbidden for the right circularly polarized laser. Obviously, in the presence of a magnetic field, this peak splits into two peaks: one at the lower frequency for $4 \to 5$ transition and another one at the upper frequency for $9 \to 10$ transition, respectively. The oscillator strength of the lowest-frequency peak is about one fourth of the lowest-frequency peak for excitation with parallel polarized light.

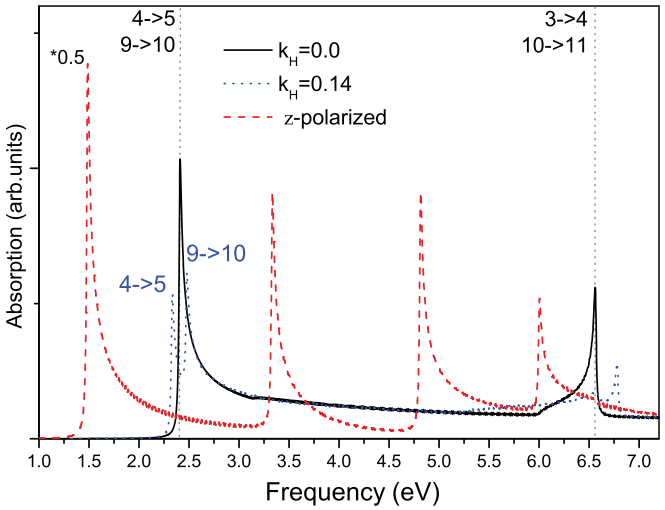


FIG. 5. (Color online) The linear absorption spectrum for right circularly polarized light for the (7, 0) tube. The black solid/blue dotted line is the result without and with magnetic field ($k_H = 0.14$), respectively. The red dashed line is one half of the parallel polarized linear absorption spectrum without magnetic field for comparison.

## V. CONCLUSION

In summary, for light with an arbitrary polarization direction with respect to the nanotube axis, we calculate the linear absorption of CNTs in the absence and presence of an axial magnetic field. On the basis of an analytic expression for the dipole matrix elements, we can analyze the contribution of every transition to the peaks in the linear absorption spectrum in a transparent way. In particular, we study the absorption spectrum for right circularly polarized laser fields. When an axial magnetic field is applied, a splitting in the nanotube's band structure occurs such that, with circularly polarized light, certain band-to-band transitions can be selectively excited.

Here, we analyze band-to-band transitions in CNTs in the absence and presence of an axial magnetic field which results in transparent easy-to-use analytical expressions. Since excitons are superpositions of band-to-band transitions, the results presented on the band structure and the optical matrix element are expected to lead to corresponding signatures in the excitonic absorption and thus should be observable. Analyzing excitonic effects requires numerical evaluations which we plan to present in a future publication.

## ACKNOWLEDGMENTS

HL is particularly grateful to Wenhui Duan at Tsinghua University for various valuable discussions, to her colleague Hong Liu, and to Guiqin Huang for helpful comments on the first draft of this article. This work is financially supported by DFG Research Training Group 1464 "Micro- and Nanostructures in Optoelectronic and Photonics", the National Natural Science Foundation of China (Grant No. 10947004), the Jiangsu Goverment Scholarship for Overseas Studies, and the Foundation of Nature and Science of Jiangsu Province in China (No. BK2008427).

[1]S. Iijima, Nature **354**, 56 (1991).
[2]E. Malić, M. Hirtschulz, F. Milde, A. Knorr, and S. Reich, Phys. Rev. B **74**, 195431 (2006).
[3]S. Motavas, A. Ivanov, and A. Nojeh, Phys. Rev. B **82**, 085442 (2010).
[4]M. F. Lin, Phys. Rev. B **62**, 13153 (2000).
[5]H. Ajiki and T. Ando, Physica B **201**, 349 (1994).
[6]R. Moradian, R. Chegel, and S. Behzad, Physica E **42**, 1850 (2010).
[7]E. Chang, G. Bussi, A. Ruini, and E. Molinari, Phys. Rev. Lett. **92**, 196401 (2004).
[8]J. Jiang, R. Saito, Ge G. Samsonidze, A. Jorio, S. G. Chou, G. Dresselhaus, and M. S. Dresselhaus, Phys. Rev. B **75**, 035407 (2007).
[9]E. Malić, J. Maultzsch, S. Reich, and A. Knorr, Phys. Rev. B **82**, 035433 (2010).
[10]T. Ando and Seiji Uryu, Phys. Status Solidi C **6**, 173 (2009).
[11]S. Uryu and T. Ando, Phys. Rev. B **83**, 085404 (2011).
[12]S. Kilina, S. Tretiak, S. K. Doom, Z. Luo, F. Papadimitrakopoulos, A. Piryatinski, A. Saxena, and A. R. Bishop, Proc. Natl. Acad. Sci. **105**, 6797 (2008).
[13]E. Malić, M. Hirtschulz, F. Milde, Y. Wu, J. Maultzsch, T. F. Heinz, A. Knorr, and S. Reich, Phys. Rev. B **77**, 045432 (2008).
[14]R. Saito, G. Dresselhaus, and M. S. Dresselhaus, Phys. Rev. B **61**, 2981 (2000).
[15]S. Reich and C. Thomsen, Phys. Rev. B **62**, 4273 (2000).
[16]F. Wang, D. J. Cho, B. Kessler, J. Deslippe, P. J. Schuck, S. G. Louie, A. Zettl, T. F. Heinz, and Y. R. Shen, Phys. Rev. Lett. **99**, 227401 (2007).
[17]Y. Miyauchi, M. Oba, and S. Maruyama, Phys. Rev. B **74**, 205440 (2006).
[18]Z. Zhang, E. Einarsson, Y. Murakami, Y. Miyauchi, and S. Maruyama, Phys. Rev. B **81**, 165442 (2010).
[19]Y. Battie, D. Jamon, J. S. Lauret, A. En Naciri, L. Broch, and A. Loiseau, Carbon **50**, 4673 (2012).
[20]M. Barkelid, G. A. Steele, and V. Zwiller, Nano Lett. **12**, 5649 (2012).
[21]J. Jiang, R. Saito, A. Grüneis, G. Dresselhaus, and M. S. Dresselhaus, Carbon **42**, 3169 (2004).
[22]Ge G. Samsonidze, A. Grüneis, R. Saito, A. Jorio, A. G. Souza Filho, G. Dresselhaus, and M. S. Dresselhaus, Phys. Rev. B **69**, 205402 (2004).
[23]S. V. Goupalov, Phys. Rev. B **72**, 195403 (2005).
[24]A. Zarifi and T. G. Pedersen, Phys. Rev. B **80**, 195422 (2009).
[25]Z. Wang, H. Zhao, and S. Mazumdar, Phys. Rev. B **76**, 115431 (2007).
[26]Y. Takagi and S. Okada, Phys. Rev. B **79**, 233406 (2009).
[27]E. Malić and A. Knorr, *Graphene and Carbon Nanotubes: Ultrafast Relaxation Dynamics and Optics* (Wiley-VCH, Berlin, 2013).
[28]H. Haug and S. W. Koch, *Quantum Theory of the Optical and Electronic Properties of Semiconductors*, 5th ed. (World Scientific, Singapore, 2009).
[29]T. B. Lynge and T. G. Pedersen, Phys. Rev. B **67**, 075206 (2003).
[30]Liu Hong and Yin Haijian, Acta Phys. Sin. **58**, 3287 (2009).
[31]S. M. Bachilo, M. S. Strano, C. Kittrell, R. H. Hauge, R. Smalley, and R. B. Weisman, Science **298**, 2361 (2002).
[32]S. Zaric, G. N. Ostojic, J. Kono, J. Shaver, V. C. Moore, and M. S. Strano, Science **304**, 1129 (2004).